

See discussions, stats, and author profiles for this publication at: <https://www.researchgate.net/publication/10828495>

3D-QSAR Studies on thieno[3,2-d]pyrimidines as Phosphodiesterase IV Inhibitors

ARTICLE *in* BIOORGANIC & MEDICINAL CHEMISTRY LETTERS · MAY 2003

Impact Factor: 2.42 · DOI: 10.1016/S0960-894X(03)00172-0 · Source: PubMed

CITATIONS

28

READS

32

4 AUTHORS, INCLUDING:



Gopalakrishnan Bulusu

TCS Innovation Labs - Hyderabad, Tata Con...

52 PUBLICATIONS 651 CITATIONS

SEE PROFILE



Pergamon

3D-QSAR Studies on Thieno[3,2-*d*]pyrimidines as Phosphodiesterase IV Inhibitors

Asit K. Chakraborti,* B. Gopalakrishnan, M. Elizabeth Sobhia and Alpeshkumar Malde

*Department of Medicinal Chemistry, National Institute of Pharmaceutical Education and Research (NIPER),
Sector-67, S.A.S. Nagar-160 062, Punjab, India*

Received 8 December 2002; revised 13 February 2003; accepted 17 February 2003

Abstract—Cyclic nucleotide phosphodiesterase IV (PDE IV) inhibitors find utility in asthma and Chronic Obstructive Pulmonary Disease (COPD) therapy. A series of 29 thieno[3,2-*d*]pyrimidines with affinity for PDE IV was subjected to three dimensional quantitative structure activity relationship (3D-QSAR) studies using comparative molecular field analysis (CoMFA) and comparative molecular similarity indices analysis (CoMSIA). Both CoMFA and CoMSIA provided statistically valid models with good correlative and predictive power. The incorporation of hydrophobic, hydrogen bond donor and hydrogen bond acceptor fields showed insignificant improvement in CoMSIA model. The 3D-QSAR models provide information for predicting the affinity of related compounds and designing more potent inhibitors.

© 2003 Elsevier Science Ltd. All rights reserved.

Introduction

Asthma is one of the most common chronic diseases worldwide and is characterized by a reversible airway obstruction, ongoing cellular inflammation, and non-specific hyperresponsiveness to a variety of challenges.¹ Acute and long term manifestations of asthma are believed to be a consequence of various inflammatory mediators released by activated inflammatory and immune cells.² During the last decade, considerable attention has been focused on cyclic nucleotide phosphodiesterase IV (PDE IV) as an attractive target for novel anti-inflammatory and anti-asthma therapy.³ There has been a spectacular evolution of the knowledge on the biochemical aspects of PDE IV as drug target and on the pharmacological and toxicological profile of its inhibitors.⁴ The inhibition of PDE IV activity increases the cellular level of cyclic adenosine 5'-monophosphate (c-AMP), thereby activating specific protein phosphorylation cascades that elicit a variety of functional responses in the inflammatory cells and bronchial smooth muscles.⁵ The mixed anti-inflammatory and bronchodilatory profile of PDE IV inhibitors could allow the discovery of new agents able to replace corticosteroids and β_2 -adrenoceptor agonists, which

represent the basis of the therapeutic management of asthma.⁶ PDE IV inhibitors are also useful in the treatment of chronic obstructive pulmonary disease (COPD).⁷

Chemically diverse classes of molecules have been reported as PDE IV inhibitors.⁸ The most studied inhibitors may be classified into three distinct chemical structural types: rolipram-related compounds, xanthine derivatives and niraquazone analogues.⁹ Although the three dimensional structure of the native PDE IV enzyme in the solid state has been recently reported,¹⁰ the experimental data on the PDE IV-inhibitor complex is not available. The structural diversity of PDE IV inhibitors suggests that the cAMP binding site represents a number of pharmacophores capable of interacting with it.¹¹ Currently, 11 compounds are in various phases of clinical trials for the treatment of asthma and COPD.¹² We report herein the results of comparative molecular field analysis (CoMFA) and comparative molecular similarity indices analysis (CoMSIA) performed on a series of thieno[3,2-*d*]pyrimidines as PDE IV inhibitors.¹³ CoMFA,¹⁴ the most popular 3D-QSAR method, has been chosen because of the renowned robustness of the model it produces.^{15,16} The CoMSIA¹⁷ method differs by the way the molecular fields are calculated and by including additional molecular fields, such as lipophilic and hydrogen bond potential. The additional fields in CoMSIA increase the significance

*Corresponding author. Tel.: +91-172-214682; fax: +91-172-214692;
e-mail: akchakraborti@niper.ac.in

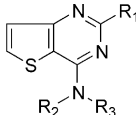
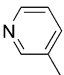
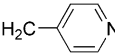
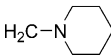
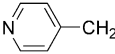
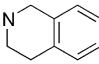
and predictive power of 3D-QSAR model and also provide better visualization and interpretation of the obtained correlation in terms of field contribution to the activity of the compound. The aim is to analyze structural requirements of this class of PDE IV inhibitors to understand the structural basis for their affinity to the catalytic center of the enzyme and to guide the design and synthesis of more potent inhibitors with pre-determined affinities.

Computational Details

Dataset for analysis

Reported in vitro data on a series of thieno[3,2-*d*]pyrimidines¹³ were used (Table 1). The IC₅₀ values of 29 molecules were segregated into groups of 23 and 6 as

Table 1. Dataset used for 3D-QSAR analyses

				
Molecule	R1	R2	R3	IC ₅₀ (μM)
1	C ₄ H ₉	H	CH ₂ Ph	0.9
2 ^a	C ₄ H ₉	H	CH ₂ Ph	1.1
3	H	H	CH ₂ Ph	14
4	C ₂ H ₅	H	CH ₂ Ph	2.3
5	CH(CH ₃)C ₂ H ₅	H	CH ₂ Ph	1.5
6	CH ₂ - <i>c</i> -C ₅ H ₉	H	CH ₂ Ph	1.1
7	CH ₂ - <i>c</i> -C ₆ H ₁₁	H	CH ₂ Ph	4.0
8	CH ₂ Ph	H	CH ₂ Ph	1.5
9	CH ₂ CH ₂ Ph	H	CH ₂ Ph	2.3
10	(CH ₂) ₄ OPh	H	CH ₂ Ph	4.7
11	Ph	H	CH ₂ Ph	3.0
12		H	CH ₂ Ph	0.6
13		H	CH ₂ Ph	1.3
14		H	CH ₂ Ph	65.0
15	C ₄ H ₉	CH ₂ -2-OCH ₃ -C ₆ H ₄	H	0.7
16	C ₄ H ₉	CH ₂ -3-OCH ₃ -C ₆ H ₄	H	1.4
17	C ₄ H ₉	CH ₂ -4-OCH ₃ -C ₆ H ₄	H	1.5
18	C ₄ H ₉	CH ₂ -2-NO ₂ -C ₆ H ₄	H	1.0
19	C ₄ H ₉	CH ₂ -3-NO ₂ -C ₆ H ₄	H	0.84
20	C ₄ H ₉	CH ₂ -2,6-diF-C ₆ H ₃	H	1.0
21	C ₄ H ₉		H	0.6
22	C ₄ H ₉	Ph	H	0.6
23	C ₄ H ₉	CH ₂ - <i>c</i> -C ₆ H ₁₁	H	1.0
24	C ₄ H ₉	-(CH ₂) ₄ -		0.6
25	C ₄ H ₉			2.7
26	C ₄ H ₉	CH ₃	CH ₂ Ph	0.8
27	C ₄ H ₉	C ₃ H ₇	CH ₂ Ph	2.5
28	C ₄ H ₉	CH ₂ Ph	CH ₂ Ph	4.0
29	C ₄ H ₉	<i>c</i> -C ₆ H ₁₁	H	0.4

^aSulfur is replaced by oxygen.

training set and test set respectively. The IC₅₀ values were converted into pIC₅₀ according to the formula,

$$\text{pIC}_{50} = -\log_{10} \text{IC}_{50}$$

Molecular modelling

The 3D-QSAR was performed using SYBYL 6.6¹⁸ installed on a Silicon Graphics Power ONYX *extreme* workstation. Since the crystal structure of PDE IV-inhibitor complex is not available, the least energy conformer was used as the bioactive conformation. The most active analogue **29** was subjected to conformational search. The minimum energy conformer subjected to further minimization. The minimized conformer, was thus obtained, was taken as the template and rest of the molecules were built from it. A constrained minimization followed by full minimization was carried out on these molecules in order to prevent the conformations moving to a false region. Tripos force field and Gasteiger-Hückel partial atomic charges were used. Powell's conjugate gradient method was used for minimization. The minimum energy difference of 0.001 kCal/mol was set as a convergence criterion.

Alignment rule

Molecule **29** was taken as the template and rest of the molecules were aligned to it using the FIT command in the SYBYL. The molecules were fitted to the template molecule by using the indole nucleus as the common sub-structure. The aligned molecules are shown in Figure 1.

CoMFA interaction energy calculation

The steric and electrostatic CoMFA fields were calculated at each lattice intersection of a regularly spaced grid of 2.0 Å in all three dimensions within defined region. The van der Waals potential and coulombic term representing the steric and electrostatic fields

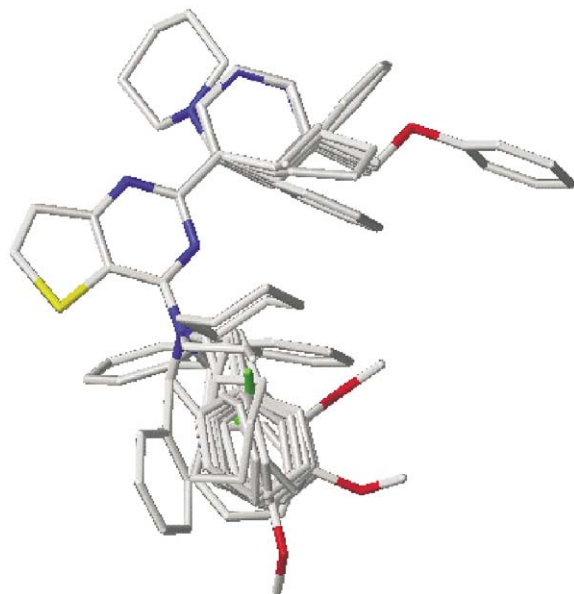


Figure 1. Alignment of the training set molecules.

respectively were calculated using standard Tripos force fields. A distance dependent dielectric constant of 1.00 was used. An sp^3 carbon atom with +1.00 charge was used as a probe atom. The steric and electrostatic fields were truncated at +30.00 kCal/mol, and the electrostatic fields were ignored at the lattice points with maximal steric interactions.

CoMSIA interaction energy calculation

The steric, electrostatic, hydrophobic, hydrogen bond donor and hydrogen bond acceptor potential fields were calculated at each lattice intersection of a regularly spaced grid of 2.0 Å. A probe atom with radius 1.0 Å and +1.0 charge with hydrophobicity of +1.0 and hydrogen bond donor and hydrogen bond acceptor properties of +1.0 was used to calculate steric, electrostatic, hydrophobic, donor and acceptor fields. The contribution from these descriptors were truncated at 0.3 kCal/mol.

Partial Least Square (PLS) analysis

PLS method was used to linearly correlate the CoMFA fields to the inhibitory activity values. The cross-validation^{19,20} analysis was performed using leave one out (LOO) method in which one compound is removed from the dataset and its activity is predicted using the model derived from the rest of the dataset. The cross validated r^2 that resulted in optimum number of components and lowest standard error of prediction were considered for further analysis. Equal weights were assigned to steric and electrostatic fields using COMFA-STD scaling option. To speed up the analysis and reduce noise, a minimum filter value σ of 2.00 kCal/mol was used. Final analysis was performed to calculate conventional r^2 using the optimum number of components.

Results and Discussion

CoMFA model obtained with 23 molecules in training set and 6 molecules in test set resulted in a cross-validated r^2 of 0.425 with minimum standard error and optimum numbers of components. The PLS statistics for CoMFA and CoMSIA are shown in Table 2. This analysis was used for final non-cross validated run, giving a correlation coefficient value of 0.996 with a low standard error of estimate giving a good linear correlation between the observed and computed affinities of the compounds in the training set. Contributions of steric and electrostatic fields are in the ratio 3:2, indicating the importance of steric fields in model generation. A plot of predicted (CoMFA) versus actual activity for training set molecules is shown in Figure 2. The test set residuals of CoMFA and CoMSIA analyses are shown in Figure 3. Figure 4 represents the plot of predicted (CoMSIA) versus actual activity values. The actual, predicted and residual values of training and test set for CoMFA and CoMSIA are given in Tables 3 and 4, respectively. Contour maps were generated as scalar product of coefficients and standard deviation associated with each CoMFA column. The 3D-QSAR

contour maps revealing the contribution of CoMFA and CoMSIA fields are shown in Figures 5 and 6 respectively. The CoMFA steric interactions are represented by green and yellow colored contours while electrostatic interactions are represented by red and blue colored contours. The bulky substituents are favored in

Table 2. Summary of CoMFA and CoMSIA statistics

Parameter	CoMFA	CoMSIA			
		S, E	S, E, H	S, E, D, A	ALL
r_{cv}^2	0.425	0.441	0.299	0.315	0.411
N	6	5	4	6	6
r^2	0.996	0.975	0.979	0.983	0.990
SEE	0.035	0.087	0.077	0.074	0.058
F-test value	708.922	132.087	210.693	153.255	251.904
Prob. of $r^2=0$	0.000	0.0	0.0	0.0	0.0
PRESS	0.46	0.68	0.46	0.81	0.75
Contributions (%)					
Steric	65.9	45.0	25.1	37.2	22.3
Electrostatic	34.1	55.0	41.6	37.0	27.8
Donor				14.2	10.2
Acceptor				11.5	11.2
Hydrophobic			33.3		28.1

r_{cv}^2 = cross-validated correlation coefficient; N = No. of components; r^2 = conventional correlation coefficient; SEE = standard error of estimate; PRESS = Predicted residual sum of squares of test set molecules, SD = Standard deviation for the test set molecules, S = steric field, E = electrostatic field, H = hydrophobic field, D = hydrogen bond donor field, A = hydrogen bond acceptor field.

CoMFA training set

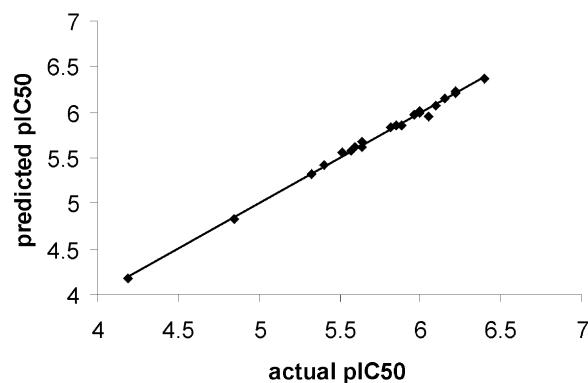


Figure 2. Plot of predicted versus actual pIC_{50} of training set molecules (CoMFA model).

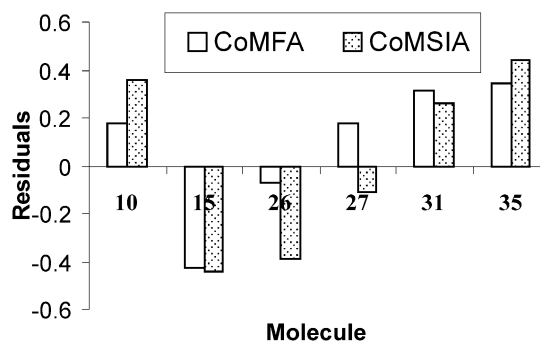


Figure 3. Histogram of residuals of the test set molecules for CoMFA and CoMSIA.

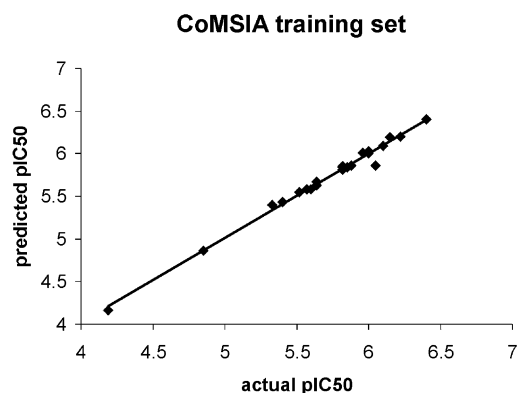


Figure 4. Plot of predicted versus actual pIC_{50} of training set molecules (CoMSIA model).

green regions and disfavored in yellow regions. The increase in positive charge is favored in blue regions while the increase in negative charge is favored in red regions. The most active molecule **29** (template) is displayed in the background of contours.

The red contours near N of the side chain as well as near the butyl side chain of the template molecule suggest incorporation of electronegative substituents for increase of the activity. This explains the better activity of **12** in which the 3-pyridyl substituent has electronegative nitrogen in appropriate position. The blue contour surrounding the terminal carbon of the butyl group of the template molecule indicates the preference for electropositive substituent. Thus, the low affinity of **10** is due to the orientation of oxygen of 4-phenoxybutyl substituent towards the unfavorable blue contour. A green contour favoring sterically bulkier substituents is seen near the terminal carbon of butyl group that par-

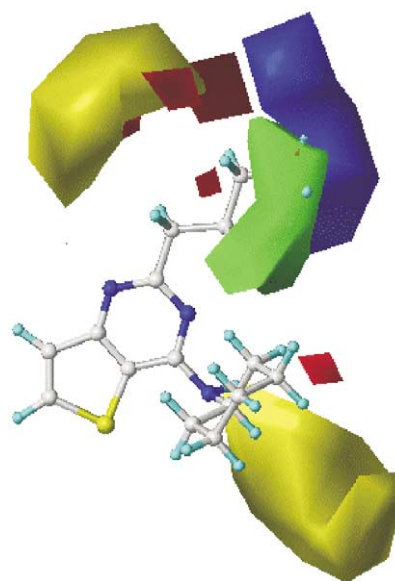


Figure 5. CoMFA STDEV*COEFF contour maps for steric and electrostatic fields. The most active molecule **29** is displayed in the background.

tially overlaps with the blue contour indicating preference for electropositive bulkier substituents. Hence, **28** exhibits less activity as two bulkier substituents on side chain N orient one of the benzyl groups towards sterically unfavorable yellow region. Furthermore, the butyl side chain is buried in unfavorable yellow region. The orientation of the butyl side chain plays an important role in modulating the activity. In **26**, **27** and **28** as the size of the substituent on N changes from methyl to propyl to benzyl; the PDE IV affinity decreases. This indicates that substituent at this position may lead to interaction with sterically unfavorable region and hence, smaller substituents are favored in this region.

The CoMSIA results were obtained using the same structural alignment and the same training and test set as defined in the CoMFA analysis. A comparative study of the data (Table 2) shows that the cross validated r^2 from CoMSIA is slightly higher than that in CoMFA for steric and electrostatic field combination. The addition of hydrophobic, hydrogen bond donor and hydrogen bond acceptor fields do not contribute significantly to the model. Among the different field combinations of CoMSIA, the all fields model has slightly lower r_{cv}^2 but higher conventional r^2 and the highest r_{cv}^2 has been

Table 3. Actual, predicted inhibitory activities (pIC_{50}) and residuals of the training set molecules

Molecule	Actual pIC_{50}	Predicted pIC_{50}		Residuals	
		CoMFA	CoMSIA	CoMFA	CoMSIA
1	6.05	5.95	5.86	0.10	0.19
3	4.85	4.83	4.86	0.02	-0.01
4	5.64	5.67	5.63	-0.03	0.01
5	5.82	5.84	5.84	-0.02	-0.02
6	5.96	5.97	6.01	-0.01	-0.05
8	5.82	5.83	5.85	-0.01	-0.03
9	5.64	5.62	5.67	0.02	-0.03
10	5.33	5.33	5.40	0.00	-0.07
11	5.52	5.56	5.55	-0.04	-0.03
12	6.22	6.24	6.20	-0.02	0.02
13	5.88	5.85	5.86	0.03	0.02
14	4.19	4.17	4.16	0.02	0.03
15	6.15	6.16	6.19	-0.01	-0.04
16	5.85	5.86	5.84	-0.01	0.01
17	5.82	5.84	5.81	-0.02	0.01
20	6.00	6.00	6.00	0.00	0.00
22	6.22	6.22	6.20	0.00	0.02
23	6.00	6.02	6.03	-0.02	-0.03
25	5.57	5.57	5.58	0.00	-0.01
26	6.10	6.07	6.09	0.03	0.01
27	5.60	5.62	5.58	-0.02	0.02
28	5.40	5.43	5.43	-0.03	-0.03
29	6.40	6.37	6.40	0.03	0.00

Table 4. Actual, predicted inhibitory activities (pIC_{50}) and residuals of the test set molecules

Molecule	Actual pIC_{50}	Predicted pIC_{50}		Residuals	
		CoMFA	CoMSIA	CoMFA	CoMSIA
2	5.96	5.79	5.60	0.18	0.36
7	5.40	5.83	5.84	-0.43	-0.44
18	6.00	6.07	6.39	-0.07	-0.39
19	6.07	5.89	6.18	0.18	-0.11
21	6.22	5.91	5.96	0.31	0.26
24	6.22	5.88	5.78	0.34	0.44

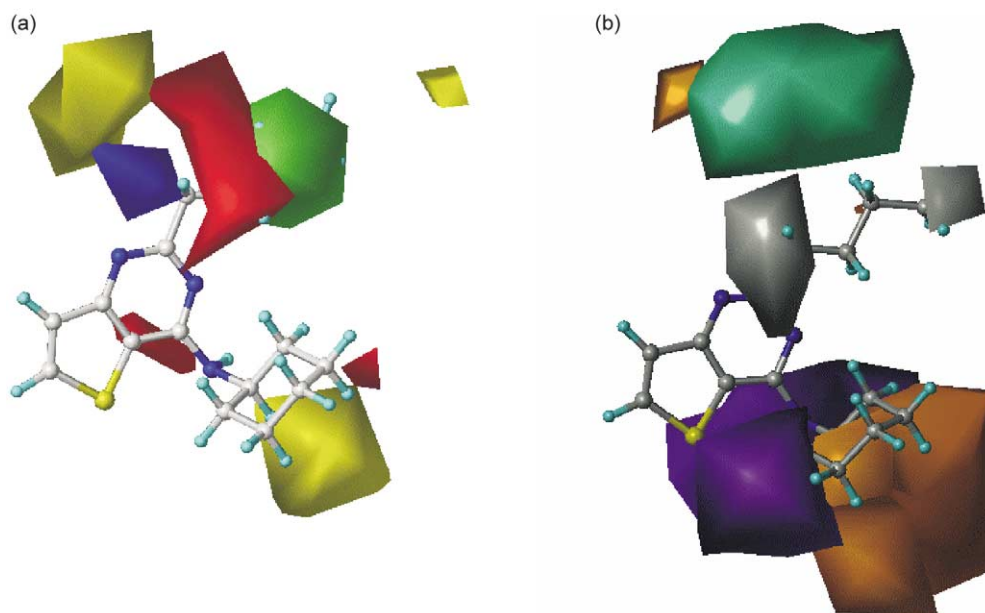


Figure 6. CoMSIA STDEV*COEFF contour maps, steric and electrostatic (a), hydrophobic, donor and acceptor (b) fields. The most active molecule **29** is displayed in the background.

obtained from combination of steric and electrostatic fields only. However, the all fields model is the one providing the most descriptive information and hence is used for the prediction of training and test set molecules. The CoMSIA model provides a linear regression plot as satisfactory as that observed in the CoMFA study (Figs. 2 and 4).

Considering the steric contours of CoMSIA, green contours indicate favorable regions while yellow contours indicate unfavorable regions for bulkier substituents. In the electrostatic contours, the introduction of electronegative substituents in red regions may increase the affinity while in blue regions decrease the affinity. In hydrophobic contours, grey regions favor hydrophobic groups while orange regions favor hydrophilic groups. The cyan and purple contours denote favorable and unfavorable regions for hydrogen bond donor groups while magenta and green-blue contours denote the favorable and unfavorable regions for hydrogen bond acceptor groups. The steric contours produced by CoMFA and CoMSIA are similar. The electrostatic contours produced by CoMSIA are different from those produced by CoMFA. CoMSIA shows an additional electronegative red contour near side chain N (Fig. 6a). The hydrophobic contours show two grey contours near the butyl side chain favoring the hydrophobic substitution (Fig. 6b). The orange contours, which disfavor the hydrophobic groups, are well compared with the steric unfavorable yellow contours generated by CoMFA and CoMSIA. In the hydrogen bond donor and hydrogen bond acceptor contours, no favorable regions are observed (Fig. 6b). The hydrogen bond donor property of the model shows unfavorable purple contour near $-NH-$ of the side chain. A green-blue contour seen above butyl group away from the ring indicates unfavorable region for hydrogen bond acceptor groups (Fig. 6b). The hydrogen bonding interactions with hetero-

aromatic nucleus and amino substituent may not be playing crucial roles in the affinity for PDE IV.

There is a statistically insignificant difference between CoMFA and final CoMSIA models indicating that incorporation of hydrophobic, hydrogen bond donor and hydrogen bond acceptor fields do not significantly contribute to the correlation.

Conclusion

3D-QSAR analysis of PDE IV inhibitors was performed to derive and compare structural requirements for PDE IV affinity. Both CoMFA and CoMSIA studies provided statistically valid models with good correlative and predictive power. The addition of hydrophobic, hydrogen bond donor and hydrogen bond acceptor fields in CoMSIA do not significantly improve the model. The analysis of CoMFA and CoMSIA contours provide the information for predicting the affinity of related compounds and for guiding the structural modifications.

References and Notes

1. Hegele, R. G. *Immunopharmacology* **2000**, 48, 257.
2. Wong, W. S.; Koh, D. *Biochem. Pharmacol.* **2000**, 59, 1323.
3. Domenico, S. *Curr. Opin. Invest. Drugs* **2000**, 1, 204.
4. Huang, Z.; Ducharme, Y.; Macdonald, D.; Robichaud, A. *Curr. Opin. Chem. Biol.* **2001**, 5, 432.
5. Beavo, J. A.; Conti, M.; Heaslip, R. J. *Mol. Pharmacol.* **1994**, 46, 399.
6. Bertrand, C. P. *Curr. Opin. Chem. Biol.* **2000**, 4, 407.
7. Perry, M. J.; Higgs, G. A. *Curr. Opin. Chem. Biol.* **1998**, 2, 472.
8. Piaz, V. D.; Giavannoni, M. P. *Eur. J. Med. Chem.* **2000**, 35, 463.
9. Christensen, S. B.; Trophy, T. J. In *Annual Reports In Medicinal Chemistry*; Hagmann, W. K., Lee, J. C., McCall, J.

- M., Plattner, J. J., Robertson, D. W., Venuti, M. C., Eds.; Academic Press: California, 1994; Vol. 29, pp 185–194.
10. Xu, R. H.; Hassel, A. M.; Vanderwaal, D.; Lambert, M.; Holmes, W.; Luther, M.; Rocque, W.; Milburn, M.; Zhaso, Y.; Ke, H.; Nolte, R. T. *Science* **2000**, 288, 1822.
11. Ducrot, P.; Andrianjara, C. R.; Wrigglesworth, R. J. *Comput-Aid. Mol. Des.* **2001**, 15, 767.
12. Burnouf, C.; Pruniaux, M. *Curr. Pharm. Des.* **2002**, 8, 1255.
13. Crepsio, M. I.; Pages, L.; Vega, A.; Segarra, V.; Lopez, M.; Domenech, T.; Miralpeix, M.; Beleta, J.; Ryder, H.; Palacios, J. J. *J. Med. Chem.* **1998**, 41, 4021.
14. Cramer, R. D.; Patterson, D. E.; Bunce, J. D. *J. Am. Chem. Soc.* **1988**, 110, 5959.
15. Desiraju, G. R.; Gopalakrishnan, B.; Jetty, R. K.; Nagaraju, A.; Raveendra, D.; Sarma, J. A.; Sobhia, M. E.; Thilagavathi, R. *J. Med. Chem.* **2002**, 45, 4847.
16. Desiraju, G. R.; Sarma, J. A.; Raveendra, D.; Gopalakrishnan, B.; Thilagavathi, R.; Sobhia, M. E.; Subramanya, H. S. *J. Phys. Org. Chem.* **2001**, 14, 481.
17. Klebe, G.; Abraham, U.; Mietzner, T. *J. Med. Chem.* **1994**, 37, 4130.
18. SYBYL 6.6, Tripos Associates Inc., 1699 S Hanley Rd., St. Louis, MO 63144, USA.
19. Cramer, R. D.; Bunce, J. D.; Patterson, D. E. *Quant. Struct.-Act. Relat.* **1988**, 7, 18.
20. Podlogar, B. L.; Ferguson, D. M. *Drug. Des. Discov.* **2000**, 17, 4.